Tempo-C_{61}: An Unusual Example of Fulleroid to Methanofullerene Conversion

Paola Ceroni,[†] Fosca Conti,[‡] Carlo Corvaja,*[,‡] Michele Maggini,[§] Francesco Paolucci,[†] Sergio Roffia,*[,†] Gianfranco Scorrano,[§] and Antonio Toffoletti[‡]

Dipartimento di Chimica G. Ciamician, Università di Bologna, Via Selmi 2, 40126 Bologna, Italy; Dipartimento di Chimica Fisica, Università di Padova, Via Loredan 2, 35131 Padova, Italy; and Dipartimento di Chimica Organica, Centro Meccanismi Reazioni Organiche-CNR, Università di Padova, Via Marzolo, 1, 35131 Padova, Italy

Received: August 17, 1999; In Final Form: October 6, 1999

An electrochemical and EPR study is reported on two isomeric C_{60} derivatives containing a covalently linked free radical TEMPO: a fulleroid and a methanofullerene. In line with other C_{60}-based nitroxide derivatives, the latter one gives a stable biradical anion upon one-electron reduction, and a metastable excited quartet state by visible light photoexcitation. Both species have characteristic EPR spectra. For the fulleroid derivative, the first reduction step is not chemically reversible and no excited state EPR signal is observed after LASER excitation. Electrochemical and spectroelectrochemical techniques indicate that fulleroid to methanofullerene conversion takes place by photoexcitation and, more interesting, upon injection of a single electron, contrary to the cases of other fulleroids so far reported.

Introduction

The addition of chemical functions to fullerenes currently represents one of the most promising strategies toward new derivatives with specific properties potentially useful for biological applications[1] or as new materials.[2] In this connection, the covalent linking of spectroscopically active probes to the fullerenes is highly desirable for studying the peculiar characteristics of important species such as fullerene anions or triplet excited states, connected with relevant fullerene features, such as superconductivity,[3] ferromagnetism,[4] optical limiting properties[5] or singlet oxygen sensitization.[6] To this end, the synthesis and EPR study of a series of fulleropyrrolidines containing the 2,2,6,6-tetramethylpiperidine-1-oxyl (TEMPO) moiety has been recently reported. These C_{60}-nitroxide derivatives could be excited by UV or visible light to a metastable quartet excited state or reduced to the corresponding biradical anion by alkali metal treatment.[7] The nitroxide unpaired electron acts as a useful probe to investigate either the kinetics and mechanism of excited quartet state formation and decay or the distribution of the added electron in the anion, along with the extent of exchange interaction between the unpaired electron on the nitroxide and that localized on the fullerene moiety.

In this paper, we report the unusual case of fulleroid **1**[8] (Chart 1), bearing the TEMPO group, which shows no paramagnetic species after both photoexcitation or alkali metal reduction. However, after photochemical, or electrochemical, conversion of **1** to the corresponding methanofullerene isomer **2**, strong transient EPR spectra of the excited quartet could be recorded upon laser irradiation, and EPR of a stable biradical monoanion could be observed after reduction with sodium metal. A combination of electrochemical and spectroelectrochemical techniques has been used to elucidate the role of the nitroxide group in the electroinduced isomerization process which, very interestingly, could be performed upon injection of a single electron.[9]

CHART 1

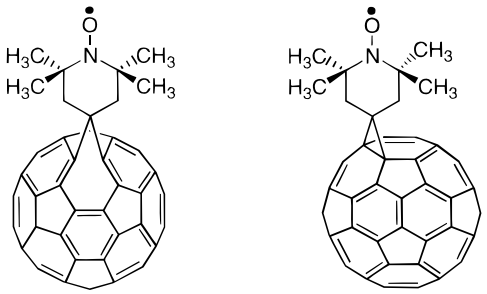

1 **2**

Experimental Section

Materials. Fulleroid (**1**) was prepared by thermal decomposition of the sodium salt of TEMPON tosylhydrazone (TEMPON = 2,2,6,6-tetramethyl-4-piperidone-1-oxyl) in the presence of C_{60}, following the procedure reported by Ishida and co-workers.[8] Methanofullerene (**2**) was obtained by irradiation of a 0.3 mM degassed *p*-xylene solution of fulleroid (**1**), with an Ar laser (1 W) at 488 nm for 8 h.

Anion Preparation. The radical anions of derivatives **1** and **2** were prepared by standard vacuum (ca. 10^{-4} mbar) techniques in a 10 mm o.d. Pyrex tube containing a few hundred micrograms of the compound. The tube was equipped with two sidearms, one being a usual EPR tube. In the second arm a sodium mirror was formed by evaporating the pure metal before tetrahydrofuran was introduced through the vacuum line. After a few freeze−pump−thaw cycles, the apparatus was sealed. The solution was carefully brought into contact with the metal mirror and the EPR spectrum was recorded after each contact.

EPR Samples Preparation. Samples for EPR measurements of neutral and photoexcited states were prepared by dissolving

[†] Università di Bologna.
[‡] Dipartimento di Chimica Fisica, Università di Padova.
[§] Centro Meccanismi Reazioni Organiche-CNR, Università di Padova.

10.1021/jp9929014 CCC: $19.00
Published on Web 12/10/1999

1 or **2** in toluene (ca. 10^{-4} M) in 4 mm o.d. quartz tubes. The samples were degassed by repeated freeze−pump−thaw cycles and sealed under vacuum.

Instrumentation. *Magnetic Resonance Measurements*. A computer-controlled Bruker ER 200D X-band spectrometer, equipped with a nitrogen flow cryostat, was employed for CW-EPR, ENDOR and time-resolved EPR measurements.

For CW-EPR experiments, a standard TE_{102} rectangular cavity with optical access was used. Because of the small line widths, 25 kHz frequency was employed to avoid the broadening of the spectral lines and the appearance of sidebands deriving from the usual 100 kHz modulation frequency.

The ENDOR spectra were recorded with a Bruker cylindrical TM_{110} cavity, using a frequency-modulated Rhode & Schwartz SMX RF signal generator, an ENI A-300 W rf power amplifier, and an EG&G 5208 two-phase lock-in analyzer. A home-written software was used to control the rf sweep and the data acquisition.

Time-resolved EPR (TR-EPR) experiments were performed using the same microwave cavity employed for CW-EPR spectra. No field modulation was used and the unmodulated signal of the microwave detector was recorded as a function of time. Therefore, a positive signal represents absorption whereas a negative one relates to emission. Transient EPR signals were collected and averaged with a LeCroy 9450A fast digital oscilloscope, synchronized with the LASER pulse. The photoexcitation was carried out by light pulses (20 ns duration, λ = 582 nm, repetition rate = 20−40 Hz) from a dye laser (Lambda Physik FL 2000, dye Rhodamine 6G) pumped by a Lambda Physik LPX 100 excimer LASER (XeCl, λ = 308 nm). Transients were collected at different magnetic field positions to obtain a surface that shows the EPR signal as a function of time and of magnetic field.

The *g* values were obtained from measurements of the microwave frequency and of the magnetic field intensity.

Electrochemical and Spectroelectrochemical Measurements. The one-compartment electrochemical cell was of airtight design with high-vacuum glass stopcocks fitted with either Teflon or Kalrez (DuPont) O-rings in order to prevent contamination by grease. The connections to the high-vacuum line and to the Schlenck tube containing the solvent were obtained by spherical joints also fitted with Kalrez O-rings. The pressure measured in the electrochemical cell, prior to trap-to-trap solvent distillation, was typically $(1-2) \times 10^{-5}$ mbar.

The working electrode was either a 0.6 mm diameter platinum wire (0.15 cm^2 approximately) sealed in glass or a Pt disk ultramicroelectrode ($r = 5\ \mu$m) also sealed in glass. The counter electrode was a platinum spiral, and the quasi-reference electrode was a silver spiral. The quasi-reference electrode drift was negligible for the time required by a single experiment. Both the counter and the reference electrodes were separated from the working electrode by ca. 0.5 cm. Potentials were measured with the ferrocene standard and are always referred to standard calomel electrode (SCE). $E_{1/2}$ values correspond to $(E_{pc} + E_{pa})/2$ from cyclic voltammetry. In some experiments, a SCE reference electrode was used, separated from the working electrode compartment by a sintered glass frit. Ferrocene was also used as an internal standard for checking the electrochemical reversibility of a redox couple.

Potential-controlled bulk electrolysis was carried out in a three-compartment electrochemical cell with both the SCE reference electrode and the platinum spiral counter electrode separated from the working electrode compartment by sintered glass frits. The working electrode was a large area platinum gauze. The electrolyzed solution was monitored at intervals during the electrolysis by steady-state voltammetry and, at the same time, UV−vis−near-IR spectra were recorded. The temperature dependence of the ferrocinium/ferrocene couple standard potential was referred to SCE by a nonisothermal arrangement, according to a reported procedure.[10]

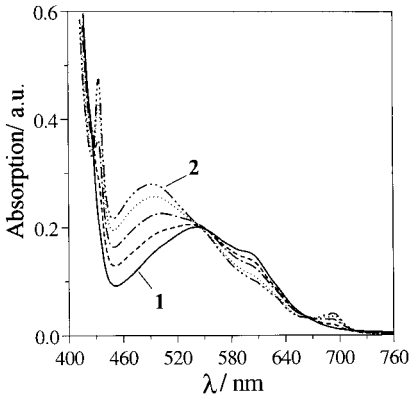

Figure 1. Visible absorption spectrum evolution during photoisomerization of a 0.3 mM *p*-xylene deareated solution of **1**, irradiated with an Ar laser beam (488 nm, 1W). Time of irradiation: (—) 0 min; (- − -) 2 h and 10 min; (− · − · −) 3 h; (···) 5 h; (− ··· − ···) 7 h and 30 min.

Voltammograms were recorded with a AMEL model 552 potentiostat or a custom made fast potentiostat[11] controlled by either a AMEL model 568 function generator or a ELCHEMA model FG-206F. Data acquisition was performed by a Nicolet model 3091 digital oscilloscope interfaced to a PC. The charge exchanged during bulk electrolysis was measured by a AMEL model 731 digital integrator. Absorption spectra were taken using a VARIAN Cary 5E UV−vis−near-IR spectrophotometer. Temperature control was accomplished within 0.1 °C with a Lauda Klein-Kryomat thermostat.

Digital Simulation of Cyclic Voltammetric Experiments. The cyclic voltammetric simulations were carried out by the DigiSim 2.1 software by Bioanalytical Systems Inc. All the electrochemical steps were considered fast in the simulation, and the chemical rate constants were chosen so as to obtain a visual best fit over a 10-fold range of scan rates.

Results

Photochemical Isomerization of Fulleroid (1). Several unsuccessful attempts to convert thermally[12−14] fulleroid (**1**) to methanofullerene (**2**)[15] prompted us to explore the photochemical rearrangement[16,17] which constitutes a convenient route to accomplish fulleroid/methanofullerene isomerization, alternative to thermal, electrochemical,[9,18] or acid-catalyzed[19] methods. Thus, a 0.3 mM solution of **1** in *p*-xylene was deaerated and irradiated with an argon laser beam (488 nm, 1 W). The isomerization reaction was monitored by UV−vis absorption spectroscopy (Figure 1). The presence of three isosbestic points at 430, 550, and 662 nm clearly indicates the interconversion between two species,[16] which was complete in ca. 8 h. The hypsochromic shift of the broad band in the visible, expected for a 58 π-electrons methanofullerene in comparison to the 60 π-electrons species **1**, whose absorption spectrum matches that of C_{60}, and the presence of two bands at 434 and 693 nm, diagnostic for methanofullerenes,[16] strongly supports the photoisomerization of **1** to methanofullerene (**2**).

EPR Measurements. *Ground State Neutral C_{60}-Nitroxides*. The continuous-wave EPR (CW-EPR) spectrum of a toluene solution of **1** has been already reported by Ishida and co-

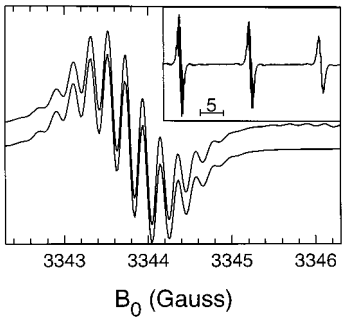

Figure 2. EPR spectrum of **1** in toluene, recorded at 300 K. The insert shows the whole spectrum, while the main picture shows the low-field lines due to the protons and their computer simulation (lower trace).

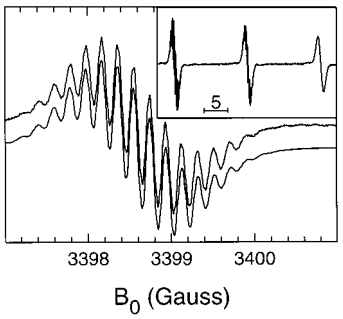

Figure 3. EPR spectrum of **2** in toluene, recorded at 300 K. The insert shows the whole spectrum, while the main picture shows the low-field lines due to the protons and their computer simulation (lower trace).

workers.[8,20] It consisted of a triplet of lines of the same intensity deriving from the ^{14}N hyperfine interaction. The lines were very broad possibly because of oxygen present in the solution. Careful preparation of a 10^{-4} M toluene solution of **1** under vacuum (10^{-4} mbar) allows the recording of a well-resolved spectrum with lines narrower than those previously reported (140 mG instead of 2.3 G, Figure 2). The additional hyperfine structure is due to the coupling of 12 equivalent protons (4 methyl groups $a_H^{CH_3} = 0.215$ G) and 4 equivalent protons (2 methylene groups $a_H^{CH_2} = 0.179$ G) of the nitroxide ring. This is illustrated by simulation of the EPR lines reported in Figure 2 (lower trace). The equivalence of the axial and equatorial methyl and methylene protons indicates a fast conformational interconversion of the six-membered ring.

A toluene solution of methanofullerene **(2)** gives a well-resolved EPR spectrum (Figure 3), which has been also calculated assuming the proton hyperfine coupling with 4 equivalent methyl groups ($a_H^{CH_3} = 0.195$ G) and with 2 equivalent methylene groups ($a_H^{CH_2} = 0.375$ G) of the nitroxide ring. This very good simulation (Figure 3, lower trace) shows that a fast conformational interconversion of the six- membered ring takes place also for derivative **2**.

The ENDOR spectra of **1** and **2**, obtained by saturating the respective low-field EPR lines, confirm the above findings. The spectra consist of three doublets of lines: two of them, at low frequency, are partially overlapped, as shown in Figure 4. The high-frequency doublet, due to the ^{14}N nuclear spin transitions and with a line separation twice the ^{14}N Larmor frequency ν_N, is centered at $a_N/2$, where a_N is the ^{14}N hyperfine splitting. The partially overlapped doublets, centered at ν_H (~14 MHz), are due to methyl and methylene protons. Notice that the ^{14}N hyperfine coupling constant of derivative **2** is larger than that observed for **1**.

Biradical Anions. The EPR spectrum of fulleroid (**1**) in tetrahydrofuran (THF) does not show significant variations

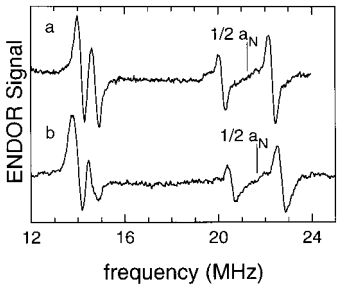

Figure 4. ENDOR spectra of toluene solutions of **1** (a) and **2** (b), recorded at 300 K. The vertical line shows the center of the pair of lines due to the ^{14}N nucleus.

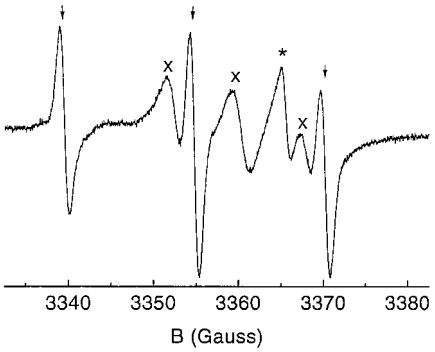

Figure 5. Room temperature EPR spectrum of **2** in MeTHF during the reduction process. The arrows indicate the hyperfine component of the neutral **2**, separated by 15.46 G. Lines marked with crosses and separated by 7.84 G are due to the biradical anion of derivative **2**. The single line marked with a star is due to a further reduction product which is the only one remaining after prolonged reduction (see text).

during the reduction with sodium metal. No evidence of a stable biradical anion is observed. Only after prolonged contact of **1** with sodium, a single narrow line at $g = 2.0001$ appears, whose relative intensity increases as the reduction process proceeds.

In contrast to fulleroid (**1**), reduction of methanofullerene (**2**) gives rise to substantial changes in the EPR spectrum. Figure 5 reports the EPR spectrum of a THF solution of **2**, recorded at room temperature, at an intermediate step of the reduction process. The spectrum is a superposition of lines due to three paramagnetic species having different g values and hyperfine splittings: a 1:1:1 triplet ($g = 2.0061$, $a_N = 15.46$ G, marked by arrows) corresponding to the neutral fullerene nitroxide radical **2**, a second 1:1:1 triplet ($g = 2.0029$, $a_N = 7.84$ G, marked by crosses) attributed to the biradical monoanion, and a single narrower line ($g = 2.0000$ marked by a star), comparable to that observed in the spectrum of fulleroid **(1)** after reduction. The single line intensity increases during the reduction process and eventually is the only one remaining after a prolonged contact with the sodium mirror as already observed for other C_{60}-nitroxide derivatives.[7d]

The hyperfine splitting constants of the neutral and reduced radicals were obtained from the computer simulation of the spectra and are reported in Table 1.

Excited States. In line with the photoinduced isomerization of fulleroid **(1)** to methanofullerene (**2**), no transient EPR signal is recorded when a toluene solution of **1** is irradiated in the EPR cavity by LASER pulses (vide infra).

On the contrary, strong transient polarized spectra could be recorded for methanofullerene (**2**) upon LASER irradiation. The complete 3D plot of the EPR signal versus magnetic field and time coordinates, obtained by laser excitation of a frozen toluene solution of **2** at $T = 150$ K, is shown in Figure 6a. The plot shows that the sign of the polarized signal changes in the

TABLE 1: *g* Factor and Isotropic Hyperfine Coupling Constants (in gauss) of Derivatives 1 and 2

compd	species[a]	*g*	a_N	$a_H^{CH_3}$	$a_H^{CH_2}$
1	n	2.0061	14.98	0.215	0.179
	ma				
	x	2.0001			
2	n	2.0061	15.46	0.195	0.375
	ma	2.0029	7.84		
	x	2.0000			

[a] n, neutral radical; ma, monoanion; x, product of further reduction.

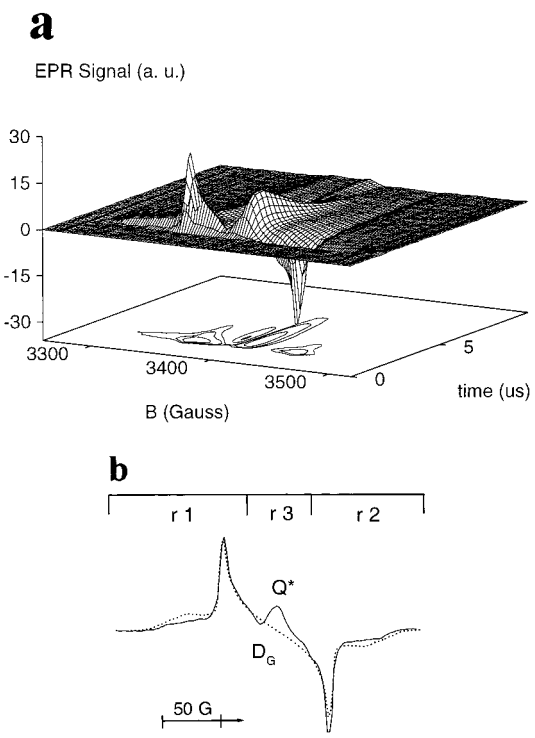

Figure 6. (a) Field-swept transient EPR signal of **2** in toluene, recorded at 150 K with microwave power of 38 mW. Positive and negative signals indicate absorptive (A), low-field part, and emissive (E), high-field part, polarizations. (b) One slice of the surface taken at a delay of 0.3 μs after the laser shot; (dotted line) computer simulation (see Table 3). Marked peaks: D_G is attributed to the electronic ground state $|-^1/_2\rangle \rightarrow |^1/_2\rangle$ transition; Q* to the $|-^1/_2\rangle \rightarrow |^1/_2\rangle$ transition of the excited quartet state.

different field regions. Figure 6b shows the slice of the surface taken at a delay of 0.3 μs after the laser pulse, together with its computer simulation (see Discussion section). The regions r1 and r2, centered at $g = 2.0021$, are symmetrical except for the sign: low-field transitions (region r1) are in enhanced absorption (A) whereas high-field transitions (region r2) are in emission (E). A series of experiments performed at $T = 50$, 80, and 120 K showed that the polarization pattern A/E in the field domain is temperature independent until $T = 50$ K.

Two distinct signals (marked with D_G and Q* in the r3 region of Figure 6b) are well resolved in the 3D plot. D_G has $g_D = 2.0061$, the same value obtained from the CW-EPR results on the ground doublet state of methanofullerene **(2)**. Q* has $g_Q = 2.0021$.

Electrochemistry. The electrochemical behavior of **2**, studied by cyclic voltammetry (CV), is first presented as its interpretation is relatively straightforward and useful to understand the more complex CV pattern of fulleroid (**1**). The CV curves for a 0.5 mM THF solution of **2** at 298 K, are shown in Figure 7.

A single, one-electron reversible oxidation peak (A) in the anodic region and five main one-electron reduction peaks,

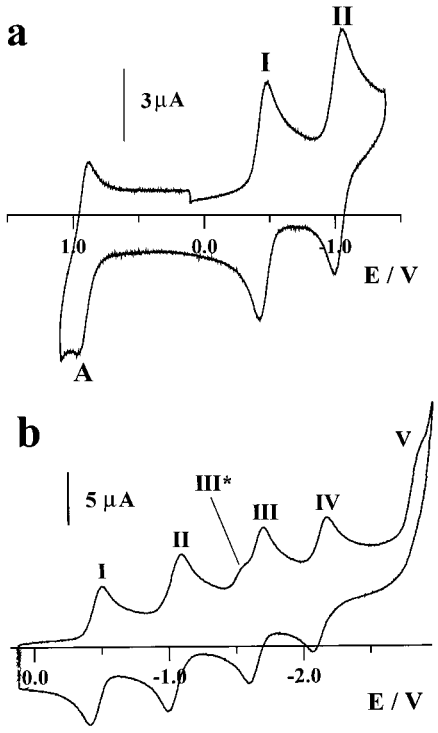

Figure 7. (a, b) CV curves of 0.5 mM **2** in THF, 0.05 M TBAH, $T = 25$ °C, $\upsilon = 0.1$ V/s. Working electrode: Pt.

TABLE 2: Half-Wave Potentials ($E_{1/2}$/V vs SCE) in THF Solution, unless Otherwise Noted,[a] at 298 K, for Compounds 1 and 2 and Pristine TEMPO

	$E_{1/2}$						
	A	I	II	III*	III	IV	V
1	+0.94	−0.42	−1.01	−1.57	−1.65	−2.12	−2.85
2	+0.95	−0.44	−1.03	−1.50	−1.64	−2.11	−2.9[a]
TEMPO	+0.85	−1.47					

[a] Irreversible process, E_{pc} value.

denoted by increasing roman numbers, are observed. A shoulder, III*****, is present in the rising part of peak III, whose anodic counterpart is not evident. While the reversibility of peaks I−IV is easily ascertained under the conditions of Figure 7, that of peak V is confirmed only at low temperatures where, however, severe distortions of the CV curve, likely due to adsorption phenomena, are detected. The $E_{1/2}$ values for the reversible processes are reported in Table 2. With the exception of peaks A and III*****, the pattern of CV curves in Figure 7 is typical of the 6,6-closed C_{61} derivatives.[9] Peaks I−V are therefore relative to the five successive reductions of fullerene moiety in **2**. Peaks A and III***** are attributed to the nitroxide group, which is known to be either oxidized or reduced under the present conditions.[21]

Fulleroid (**1**) shows a strikingly different CV behavior compared to **2** under the same conditions. The CV curve for a 0.5 mM THF solution of **1** at 298 K is shown in Figure 8a.[22] The $E_{1/2}$ values for the redox processes relative to **1** are reported in Table 2.

In the CV of **1**, five reduction peaks are observed. In contrast to derivative **2**, however, (i) peak I lacks its anodic counterpart, (ii) the shoulder III* is missing, and (iii) peak IV corresponds to a two-electron charge transfer (see also Figure 8b). In addition, peak IV has a shoulder (IV*****) in its rising part. Figure 8b also shows the one-electron wave (A) relative to the nitroxide reversible oxidation. Peak IV*−IV consists of two consecutive one-electron reduction processes that occur at slightly different

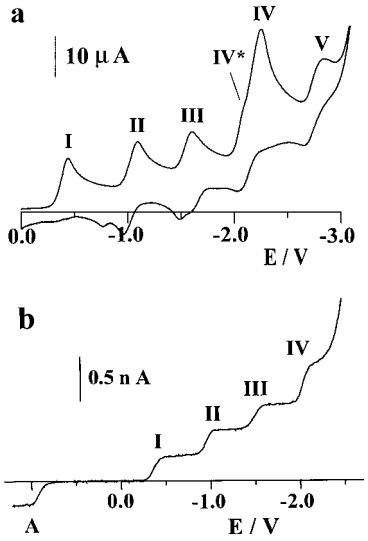

Figure 8. (a) CV curves of 0.5 mM **1** in THF, 0.05 M TBAH, $T = 25$ °C, $\upsilon = 0.1$ V/s. (b) Steady-state voltammetric curve of 0.5 mM **1** in THF, 0.05 M TBAH, $T = 25$ °C, $\upsilon = 0.01$ V/s. Working electrode: Pt. In (b) a Pt disk UME (diameter 10 μm) was used.

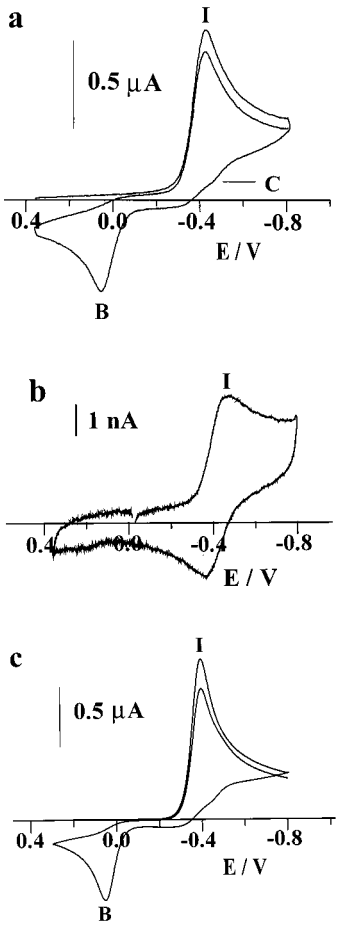

Figure 9. CV curve of 0.5 mM **1** in THF, 0.05 M TBAH, $T = 25$ °C, $\upsilon = 0.1$ V/s. (b) As (a) $\upsilon = 200$ V/s; Working electrode: Pt. A Pt disk UME (diameter 10 μm) was used in b). (c) Simulated CV curve, under the conditions of (a), calculated according to the mechanism of Scheme 1.

potentials. Furthermore, in the reverse scan, only a one-electron oxidation peak is found as the anodic partner of peak IV*−IV.

The CV curve reported in Figure 9a, obtained under the conditions of Figure 8a but with the cathodic scan limited to the first process, confirms that peak I is irreversible. In addition,

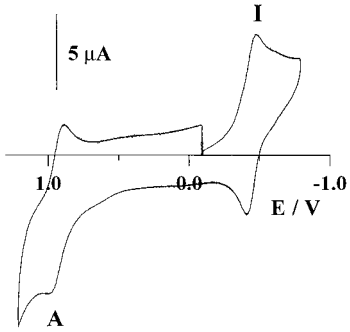

Figure 10. CV curve of bulk electrolysis product (after its electrochemical reoxidation). Concentration is approximately 0.25 mM in 0.025 M TBAH THF solution. $T = 25$ °C, $\upsilon = 0.1$ V/s. Working electrode: Pt.

an irreversible oxidation peak (B), with $E_{pa} = 0.10$ V ($\upsilon = 0.2$ V/s), appears during the anodic scan.

By either increasing the scan rate or lowering the temperature, peak I gradually attains reversibility, the i_{pa}/i_{pc} ratio approaching unity at $\upsilon \geq 200$ V/s, with $E_{1/2} = -0.42$ V (Figure 9b). Concomitantly, as peak I gains reversibility, peak B decreases, eventually disappearing when full reversibility of I is attained. A minor feature in the CV curve of Figure 9a is the presence of the small shoulder C at ca. −0.46 V in the reverse scan curve. This observation will become important in connection with the results of bulk electrolysis (vide infra).

Spectroelectrochemistry. A 0.5 mM solution of **1** (0.05 M TBAH, 25 °C) is electrolyzed at −0.6 V, which allows the first reduction process (Figure 8, peak I). Absorption spectra are recorded periodically during the electrolysis, following the appearance and increase of the typical $C_{60}^{\bullet -}$ NIR band at 1125 nm.

After one electron/molecule reoxidation, the electrolyzed solution is checked by CV (Figure 10). Quite surprisingly, the first reduction process, irreversible before electrolysis, becomes reversible ($E_{1/2} = -0.44$ V), and both the overall CV pattern (including oxidation and reduction peaks of TEMPO) and the UV−vis absorption spectrum shows a close similarity to those recorded for **2**.

Therefore, it is reasonable to presume that, under the above bulk electrolysis conditions, the isomerization of fulleroid (**1**) to methanofullerene (**2**) takes place, as discussed in the following section.

Discussion

Ground state EPR spectra of neutral **1** and **2** are typical of nitroxide radicals with the exception of an unusually small line width (≤150 mG) that causes a well-resolved proton hyperfine structure (Figures 2 and 3). Table 1 shows proton and ^{14}N hyperfine splitting constants for derivatives **1** and **2**. While the methyl protons hyperfine couplings for isomers **1** and **2** are very similar, the methylene protons coupling of **2** is about twice larger than that of **1**. The most relevant structural difference between the two isomers is that in **1** the carbon atom, to which the TEMPO moiety is spiro-linked, is part of a 1,10-annulene-like structure,[23] whereas in methanofullerene (**2**) the same atom is part of a more strained cyclopropane ring. The hybridization at that carbon is also different, producing the observed methylene protons splitting difference. On the other hand, the origin of the moderate shift of the electron spin density from oxygen to nitrogen in derivative **2** relative to **1** (3% increase of ^{14}N hyperfine constant) is not clear. To the best of our knowledge,

SCHEME 1

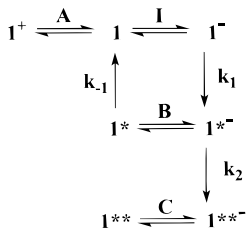

this is the first example of an effect on the nitrogen coupling of a substitutent in position 4 of the TEMPO ring.

Derivative **1** does not show a stable biradical anion in the EPR measurements. The observation is in agreement with the CV results that indicate a monoelectronic and reversible first reduction peak (see Figures 7b and 9a) only for methanofullerene (**2**). The EPR spectrum of derivative **2** biradical anion, obtained in THF by reduction with sodium metal, is similar to that of fulleropyrrolidine nitroxide (FPNO) anions[7d] (Figure 5). It consists of three lines with ^{14}N hyperfine separation, a_N, one-half of that recorded for the neutral radical. This is expected if the electron exchange interaction J is much larger than the nitrogen hyperfine coupling constant.[24,25] The g factor of the anion radical of **2** corresponds to the average between the g value of radical anion of C_{60}, or of C_{60} monoadducts such as *N*-methylfulleropyrrolidine ($g_{FP} = 1.9999$),[26] and the g value of the nitroxide free radical ($g_{FPNO} = 2.0061$). This is expected as the exchange interaction averages two limiting situations: the whole unpaired electron distributed only on the fullerene, and the unpaired electron localized on the nitroxide group.

If the contact of **2** with sodium metal is prolonged, only a single line can be recorded in the EPR spectrum. This line is also observed for **1** under the same conditions (see Table 1).

The origin of this single line as well as the absence of the anion three-line spectrum of **1** can be interpreted by considering in detail the electrochemical characterictics of **1** and **2**.

The CV behavior relative to the first reduction of **1** can be rationalized in the frame of the square mechanism illustrated in Scheme 1. A moderately fast, irreversible chemical reaction involves $\mathbf{1}^-$, and generates a new electroactive species ($\mathbf{1^{*-}}$) which is reoxidized to **1*** (peak B, Figure 9a).

A fast follow-up reaction, coupled to reoxidation B, repristinates **1**. Notice that the height of peak I in the second scan (Figure 9a), performed without renewing the diffusion layer, is close enough to that in the first scan, thus confirming the back-conversion of **1*** to **1**. The shoulder C, Figure 9a, only observed at rather low scan rates, indicates the occurrence of a slow chemical process which converts $\mathbf{1^{*-}}$ to the new species $\mathbf{1^{**-}}$, whose oxidation is in turn responsible for shoulder C. This mechanism is confirmed by performing the digital simulation of the CV curves, under the conditions of Figure 9a,b. In the simulations, Nernstian redox processes and first-order chemical reactions are assumed. The latter assumption comes from the observed concentration-independent CV behavior. A very good agreement between simulated and experimental curves is obtained (Figure 9c). The experimental $E_{1/2}$ value is used for the $\mathbf{1}/\mathbf{1}^-$ redox couple whereas those for the remaining couples are obtained from simulations: $E_{1/2}(\mathbf{1^*}/\mathbf{1^{*-}}) = +0.10$ V; $E_{1/2}(\mathbf{1^{**}}/\mathbf{1^{**-}}) = -0.44$ V. The rate constant values for the chemical step in Scheme 1 are $k_1 = 200\ s^{-1}$, $k_{-1} = 400\ s^{-1}$, and $k_2 = 0.03\ s^{-1}$, respectively. Digital simulation of the CV curves, obtained over the range 213−298 K, gives an Arrhenius activation energy of 17 ± 3 kcal/mol for the $\mathbf{1}^- \rightarrow \mathbf{1^{*-}}$ reaction.

As anticipated above, the CV pattern observed for **1** at high scan rates and/or low temperatures (≤240 K) is similar to that of **2**. As peak I attains more and more reversible features, peak IV*−IV gradually passes from a two-electron to a one-electron peak. Concomitantly, a shoulder III* on the rising part of peak III, already attributed to nitroxide reduction in **2**, gradually appears. Quite interestingly, the irreversibility of peak I (fullerene-centered) and the double height of peak IV on the one hand and the observation of peak III* (reduction of nitroxide group) on the other are mutually exclusive phenomena. This strongly suggests that the nitroxide group plays a fundamental role in the unusual CV behavior of fullerene moiety in **1**. It has to be stressed that such a behavior is not observed in the case of both **2** and FPNOs studied under the same conditions.

The coincidence of both CV patterns, $E_{1/2}$ values, and UV−vis absorption spectrum of the reoxidized bulk electrolysis product with those of **2** demonstrates that, in the long time scale of electrolysis, the fulleroid-to-methanofullerene isomerization takes place upon reduction of **1**, and that **1**** has to be identified as the species **2**. It is worth noting that this is the first example of electrochemical valence-bond isomerization of a fulleroid to a methanofullerene occurring upon injection of a single electron.[9]

Identification of Intermediate 1*. CV features, similar to those observed for **1**, have been reported in the case of the electrochemical reduction of some spiroannulated methanofullerenes containing either the 1,1-(4-oxocyclohexa-2,5-dieno)- or the 9,9-fluorenyl group, the latter bearing electron-withdrawing groups.[27] The CV curves reported for the above-mentioned compounds, at 25 °C and slow scan rates, show a close resemblance to those reported here for derivative **1**. In particular, the first reduction is irreversible. A ring-opening mechanism is proposed, also supported by quantum-chemical calculations, based on the occurrence of through-space interactions between the p_z orbitals of the fullerene carbon atoms in the two rings adjacent to the bridge and the p_z orbitals in the cyclopentadienyl or hexadienyl ring of the addend (periconjugation). In those cases in which such interactions cannot occur, as for instance in the saturated 1,1-(4-oxycyclohexano)fullerene, a reversible CV behavior is expected and actually observed, for both 5,6 and 6,6 isomers.[27] It is worth noting that the latter species are structurally and electronically closely related to **1** and **2**, respectively, and a reversible CV behavior would therefore be analogously expected for these compounds. This expectation is only met experimentally in the case of **2**. For the absence of possible periconjugation stabilization, the hypothesis that the kinetic complications observed in the reduction of **1** may be ascribed to a simple ring-opening mechanism is therefore not easily tenable. Intervention of nitroxide group in the stabilization of the open form, with the formation of a covalent bond via a radical−radical coupling between nitroxide oxygen and a bridgehead carbon atom, could, however, be invoked.[28] The presence in the fullerene moiety of this new bond, with an electron-withdrawing oxygen atom linked to the fullerene cage, may also explain the large anodic shift of **1*** reduction with respect to **1** (+0.10 vs −0.42 V). Because of its participation in the new bond, nitroxide would be electrochemically inactive, thus explaining why, when peak I is irreversible, peak III* is absent. At the same time, the double height of peak IV, observed under the same conditions, would define the cathodic limit of stability of such an intermediate: the injection of the fourth electron (fullerene-centered peak IV) would bring about the cleavage of the C−O bond in $\mathbf{1^{*4-}}$. The released nitroxide would be immediately reduced at this potential (peak IV*), much more negative than the corresponding $E_{1/2}$ (−1.47 V). Finally, peak V would correspond to the further reduction of this open species.

In the reverse scan, reoxidation of reduced free nitroxide would occur at potentials close to the corresponding $E_{1/2}$: this may explain the splitting of the anodic partner of peak III (Figure 8a). On the other hand, the absence of the anodic partner of peak I and the presence of peak B, under the conditions of Figure 8a, suggests that, when the third electron is removed, the C−O bond would form again, repristinating **1***. Some degradation is also likely to occur at very negative potentials for the presence of minor peaks in the reverse scan, not further identified.

In view of the CV behavior of fulleroid **1**, as depicted in Scheme 1, the absence of EPR signal for reduced **1** is not surprising. In fact, neither $\mathbf{1}^-$ nor $\mathbf{1}^{*-}$ is expected to be observed via EPR for their too short lifetimes. However $\mathbf{1}^{**-}$ (i.e., $\mathbf{2}^-$), which is the stable species forming from $\mathbf{1}^-$ on a longer time scale, is EPR active (vide supra). The fact that no EPR response is instead obtained upon reducing **1** may be explained assuming that, under the reducing conditions used for the preparation of anions in the EPR experiments (i.e., Na/THF, see Experimental Section), and in the time scale of EPR experiments, $\mathbf{2}^-$ is not formed but rather a degradation product in turn responsible for the single line in the EPR spectrum is obtained.

Finally, the fact that, in contrast to **2**, no TR-EPR spectra are observed for **1** has to be related to the photoinstability of the latter. Because of their similarity, the electronic states of **1** and **2** can be discussed with reference to those of FPNOs.[7b] We have shown that FPNOs can be excited by UV or visible light to a doublet excited state that can be described as a singlet electronically excited fullerene bonded to a ground state nitroxide. From this state, FPNOs convert by intersystem crossing (ISC) into two lower energy states. These states correspond to a triplet C_{60} linked to the nitroxide. According to the two spin angular momenta S (on the fullerene) and σ (on the nitroxide), the two excited states are a doublet D* and a quartet Q*. In the latter, S and σ are parallel ($S_{tot} = {}^3/_2$), while in the D* state S and σ are antiparallel ($S_{tot} = {}^1/_2$).

For **1** and **2** the same type of excited states is expected. Q* has long lifetime because its spin multiplicity is different from that of the ground state. It can be detected with TR-EPR. Moreover, also the electronic ground state D_G can be detected by TR-EPR because it becomes spin polarized. Nevertheless, TR-EPR spectra are recorded only for **2** (see Figure 6). This is what one expects for the presence of a photoisomerization process converting **1** into **2**.

The laser excitation produces in fact the breaking of a bond in **1** between the TEMPO group and the fullerene moiety. Consequently, the absence of TR-EPR signals for **1** could be explained by a rapid deactivation of the quartet state with the formation of the new species.

The observed polarization pattern can be explained by the following considerations. There are two different mechanisms of ISC. For one of them, promoted by spin−orbit coupling, a spectrum is generated in enhanced absorption at low field and in emission at high field (A/E), or vice versa (E/A) depending on the selectivity of the populating rates of the zero-field triplet sublevels.[29] This mechanism predicts a nonpolarized $(Q^*)_{-1/2} \rightarrow (Q^*)_{1/2}$ transition of the excited quartet state. For the other one, radical triplet pair mechanism (RTPM)[30], a spectrum completely in enhanced absorption or in emission is produced. The polarization character depends on the exchange interaction J between the nitroxide electron and the unpaired electrons on the excited fullerene moiety. J separates the energy of the D* and Q* states, and its sign determines the absorptive or emissive signal. The RTPM is responsible for the polarization of the central line, $(Q^*)_{-1/2} \rightarrow (Q^*)_{1/2}$, of the excited quartet state and of the polarization of the ground state D_G. The 3D plot of Figure 6a points out a mixing of the two different mechanisms. Nevertheless, the RTP mechanism contribution to ISC is smaller than that due to spin−orbit coupling.

TABLE 3. Zfs Parameters (in gauss), ^{14}N Hyperfine Tensor (in gauss), and Populating Rates Used To Reproduce EPR Spectrum of Quartet State 2 in Toluene Solution at $T = 150$ K (See Figure 6b)

$D/g\beta$	$E/g\beta$	A_{xx}	A_{yy}	A_{zz}	$(p_x - p_z):(p_y - p_z)$
47	0	2	2	11	0.77:0.97

The time evolution of the EPR signals of D_G and of Q* is different. Therefore, it is possible to choose a time delay after the LASER pulse where one transition is almost neglectable. The spectrum shown in Figure 6b corresponds to a condition where the electronic doublet ground state $(D_G)_{-1/2} \rightarrow (D_G)_{1/2}$ transition (peak marked with D_G) is almost zero and the excited quartet state $(Q^*)_{-1/2} \rightarrow (Q^*)_{1/2}$ transition (peak marked with Q*) has low intensity.

The spectral features are well reproduced by a spectrum calculated taking into account the zero field splitting tensor, the ^{14}N hyperfine tensor, and the populating rates of the zfs triplet sublevels (see Table 3 and the dotted line in Figure 6b). Details of the simulation program together with a detailed discussion on the relevant polarization mechanisms will be published elsewhere.

Conclusion

TEMPO methanofullerene (**2**) has the same electrochemical behavior as other C_{60} adducts containing a covalently linked nitroxide. In particular, its first CV peak corresponds to a reversible one-electron reduction process, producing the biradical anion. Moreover, upon visible light photoexcitation, **2** gives the transient EPR signal of the metastable quartet state, corresponding to a triplet excited fullerene coupled with the nitroxide unpaired spin. Fulleroid (**1**) isomerizes to **2** by one-electron reduction at the potential of the first CV peak. This is the first observation of a fulleroid to methanofullerene conversion upon injection of a single electron. Fast photochemical isomerization is responsible of the lack of the excited state EPR signal for derivative **1**.

Acknowledgment. We thank Dr. R. Seraglia (CNR-Padova) for MALDI-MS data. We are indebted to Prof. M. Prato for helpful discussions. This work was in part supported by CNR through the Centro Stati Molecolari Radicalici ed Eccitati and Centro Meccanismi Reazioni Organiche (legge 95/95), by MURST (contract No. 9803194198), and by the University of Bologna (Funds for Selected Research Topics).

References and Notes

(1) (a) Jensen, A. W.; Wilson, S. R.; Schuster, D. I. *Bioorg. Med. Chem.* **1996**, *4*, 767−779. (b) Da Ros, T.; Prato, M. *Chem. Commun.* **1999**, 663−669.

(2) (a) Mirkin, C. A.; Caldwell, W. B. *Tetrahedron* **1996**, *52*, 5113−5130. (b) Prato, M. *J. Mater. Chem.* **1997**, *7*, 1097−1109.

(3) Hebard, A. F.; Rosseinski, M. J.; Haddon, R. C.; Murphy, D. W.; Glarum, S. H.; Palstra, T. T. M.; Ramirez, A. P.; Kortan, A. R. *Nature* **1991**, *350*, 600−601.

(4) Allemand, P. M.; Khemani, K. C.; Koch, A.; Wudl, F.; Holczer, K.; Donovan, S.; Gruner, G.; Thompson, J. D. *Science* **1991**, *253*, 301−303.

(5) Tutt, L. W.; Kost, A. *Nature* **1992**, *356*, 225−226.

(6) Foote, C. S. *Top. Curr. Chem.* **1994**, *169*, 347−363.

(7) (a) Corvaja, C.; Maggini, M.; Prato, M.; Scorrano, G.; Venzin, M. *J. Am. Chem. Soc.* **1995**, *117*, 8857−8858. (b) Corvaja, C.; Maggini, M.; Ruzzi, M.; Scorrano, G.; Toffoletti, A. *Appl. Magn. Reson.* **1997**, *12*, 477−493. (c) Mizuochi, N.; Ohba, Y.; Yamauchi, S. *J. Phys. Chem. A* **1997**,

101, 5966−5968. (d) Arena, F.; Bullo, F.; Conti, F.; Corvaja, C.; Maggini, M.; Prato, M.; Scorrano, G. *J. Am. Chem. Soc.* **1997**, *119*, 789−795. (e) Li, Y.; Mao, Z.; Xu, J.; Yang, J.; Guo, Z.; Zhu, D.; Li, J.; Yin, B. *Chem. Phys. Lett.* **1997**, *265*, 361−364. (f) Li, Y. L.; Xu, J.-H.; Zheng, D.-G.; Yang, J.-K.; PAn, C.-Y.; Zhu, D.-B. *Solid State Commun.* **1997**, *101*, 123−128. (g) Zheng, D.-G.; Li, Y.-L.; Mao, Z.; Zhu, D.-B. *Synth. Commun.* **1998**, *28*, 879−886. (h) Matsuda, K.; Ulrich, G.; Iwamura, H. *J. Chem. Soc., Perkin Trans. 2* **1998**, 1581−1588.

(8) Ishida, T.; Shinozuka, K.; Nogami, T.; Kubota, M.; Ohashi, M. *Tetrahedron* **1996**, *52*, 5103−5112.

(9) Echegoyen, L.; Echegoyen, L. E. *Acc. Chem. Res.* **1998**, *31*, 593−601.

(10) Yee, E. L.; Cave, R. J.; Guyer, K. L.; Tyma, P. D.; Weaver, M. J. *J. Am. Chem. Soc.* **1979**, *101*, 1131−1137.

(11) Amatore, C.; Lefrou, C.; Pflüger, F. *J. Electroanal. Chem.* **1989**, *270*, 43−59.

(12) Suzuki, T.; Li, Q.; Khemani, K. C.; Wudl, F. *J. Am. Chem. Soc.* **1992**, *114*, 7301−7302.

(13) Diederich, F.; Isaacs, L.; Philp, D. *Chem. Soc. Rev.* **1994**, *23*, 243−255.

(14) Paolucci, F.; Marcaccio, M.; Roffia, S.; Orlandi, G.; Zerbetto, F.; Prato, M.; Maggini, M.; Scorrano, G. *J. Am. Chem. Soc.* **1995**, *117*, 6572−6580.

(15) A prolonged heating of the reaction mixture in 1,2-dichlorobenzene gave mostly untractable materials.

(16) Janssen, R. A. J.; Hummelen, J. C.; Wudl, F. *J. Am. Chem. Soc.* **1995**, *117*, 544−545.

(17) Li, Z.; Shevlin, P. B. *J. Am. Chem. Soc.* **1997**, *119*, 1149−1150.

(18) Eiermann, M.; Wudl, F.; Prato, M.; Maggini, M. *J. Am. Chem. Soc.* **1994**, *116*, 8364−8365.

(19) González, R.; Hummelen, J. C.; Wudl, F. *J. Org. Chem.* **1995**, *60*, 2618−2620.

(20) Ishida, T.; Shinozuka, K.; Kubota, M.; Ohashi, M.; Nogami, T. *J. Chem. Soc., Chem. Commun.* **1995**, 1841−1842.

(21) Serve, D. *Electrochim. Acta* **1975**, *20*, 469−477.

(22) Only at 240 K it was possible to obtain a CV pattern similar to that shown for derivative **2**.

(23) Vogel, E. *Pure Appl. Chem* **1982**, *54*, 1015.

(24) Luckhurst, G. R. *Biradical as Spin Probes*, in *Spin Labeling—Theory and Applications*; Berliner, L. J., Ed.; Academic: New York, 1976; Chapter 4, p 133.

(25) Rozantsev, E. G. *Free Nitroxyl Radicals*; Plenum: New York, 1970.

(26) Brustolon, M.; Zoleo, A.; Agostini, G.; Maggini, M. *J. Phys. Chem.* **1998**, *102*, 6331−6339.

(27) Eiermann, M.; Haddon, R. C.; Knight, B.; Li, Q. C.; Maggini, M.; Martin, N.; Ohno, T.; Prato, M.; Suzuki, T.; Wudl, F. *Angew. Chem., Int. Ed. Engl.* **1995**, *34*, 1591−1594.

(28) The proposed structure of $\mathbf{1}^{*-}$ could not be demonstrated. However, the mechanism of its formation, involving ring opening and subsequent rearrangement, is compatible with the measured 17 kcal mol^{-1} activation energy. This compares well with reported activation energy values for similar fulleroid to methanofullerene rearrangements (ref 17 and Wallenborn, E.-U.; Haldimann, R. F.; Klaerner, F.-G.; Diederich, F. *Chem. Eur. J.* **1998**, *4*, 2258−2265).

(29) Atherton, N. M. *Principles of Electron Spin Resonance*; Ellis Horwood PTR Prentice Hall: New York, 1993.

(30) (a) Blättler, C.; Jent, F.; Paul, H. *Chem. Phys. Lett.* **1990**, *166*, 375−380. (b) Kawai, A.; Obi, K. J. *Phys. Chem.* **1992**, *96*, 5701−5704.